

Pressure-induced structural transitions and metallization in $ZrSe_2$

Yiping Gao(高一平), Chenchen Liu(刘晨晨), Can Tian(田灿), Chengcheng Zhu(朱程程), Xiaoli Huang(黄晓丽), and Tian Cui(崔田)

Citation: Chin. Phys. B, 2024, 33 (**12**): 126104. DOI: 10.1088/1674-1056/ad8ec9
Journal homepage: http://cpb.iphy.ac.cn; http://iopscience.iop.org/cpb

What follows is a list of articles you may be interested in

Pressure-induced structural, electronic, and superconducting phase transitions in $TaSe_3$

Yuhang Li(李宇航), Pei Zhou(周佩), Chi Ding(丁驰), Qing Lu(鲁清), Xiaomeng Wang(王晓梦), and Jian Sun(孙建)
Chin. Phys. B, 2024, 33 (**10**): 106102. DOI: 10.1088/1674-1056/ad6f92

Ultrafast dynamics in photo-excited Mott insulator $Sr_3Ir_2O_7$ at high pressure

Xia Yin(尹霞), Jianbo Zhang(张建波), Wang Dong(王东), Takeshi Nakagawa, Chunsheng Xia(夏春生), Caoshun Zhang(张曹顺), Weicheng Guo(郭伟程), Jun Chang(昌峻), and Yang Ding(丁阳)
Chin. Phys. B, 2024, 33 (**1**): 016103. DOI: 10.1088/1674-1056/acdc8c

Structural stability and ion migration of Li_2MnO_3 cathode material under high pressures

Ze-Ren Xie(谢泽仁), Si-Si Zhou(周思思), Bei-Bei He(贺贝贝), Huan-Wen Wang(王欢文), Yan-Sheng Gong(公衍生), Jun Jin(金俊), Xiang-Gong Zhang(张祥功), and Rui Wang(汪锐)
Chin. Phys. B, 2023, 32 (**12**): 126101. DOI: 10.1088/1674-1056/ace2b1

Prediction of superionic state in LiH_2 at conditions enroute to nuclear fusion

Fude Li(李福德), Hao Wang(王豪), Jinlong Li(李津龙), and Huayun Geng(耿华运)
Chin. Phys. B, 2023, 32 (**10**): 106103. DOI: 10.1088/1674-1056/acea68

Pressure-induced stable structures and physical properties of Sr-Ge system

Shuai Han(韩帅), Shuai Duan(段帅), Yun-Xian Liu(刘云仙), Chao Wang(王超), Xin Chen(陈欣), Hai-Rui Sun(孙海瑞), and Xiao-Bing Liu(刘晓兵)
Chin. Phys. B, 2023, 32 (**1**): 016101. DOI: 10.1088/1674-1056/ac6db5

SPECIAL TOPIC — Structures and properties of materials under high pressure

Pressure-induced structural transitions and metallization in $ZrSe_2$

Yiping Gao(高一平)[1,†], Chenchen Liu(刘晨晨)[1,†], Can Tian(田灿)[1], Chengcheng Zhu(朱程程)[1], Xiaoli Huang(黄晓丽)[1,‡], and Tian Cui(崔田)[2]

[1] *State Key Laboratory of Superhard Materials, College of Physics, Jilin University, Changchun* 130012, *China*
[2] *School of Physical Science and Technology, Ningbo University, Ningbo* 315211, *China*

(Received 27 September 2024; revised manuscript received 27 October 2024; accepted manuscript online 5 November 2024)

High-pressure studies of two-dimensional materials have revealed numerous novel properties and physical mechanisms behind them. As a typical material of transition metal dichalcogenides (TMDs), $ZrSe_2$ exhibits high carrier mobility, rich electronic states regulated by doping, and high potential in applications at ambient pressure. However, the properties of $ZrSe_2$ under pressure are still not clear, especially for the structural and electrical properties. Here, we report the investigation of $ZrSe_2$ under pressure up to 66.5 GPa by *in-situ* x-ray diffraction, Raman, electrical transport measurements, and first-principles calculations. Two structural phase transitions occur in $ZrSe_2$ at 8.3 GPa and 31.5 GPa, from $P\text{-}3m1$ symmetry to $P2_1/m$ symmetry, and finally transformed into a non-layer $I4/mmm$ symmetry structure. Pressure-induced metallic transition is observed at around 19.4 GPa in phase II which aligns well with the results of the calculation. Our work will help to improve the understanding of the evolution of the structure and electrical transport properties of two-dimensional materials.

Keywords: high pressure, transition metal dichalcogenides, structure phase transition, electrical transport properties

PACS: 61.05.cp, 61.50.Ks, 64.30.–t, 78.30.–j **DOI:** 10.1088/1674-1056/ad8ec9

1. Introduction

Since the discovery of graphene,[1] band engineering has been a focus in research on two-dimensional (2D) materials[2–4] due to the inherent zero band gap limitation of graphene. To get an enhancement of the electrical, optical, and structural properties, pressure engineering has become one of the most commonly applied methods in 2D material research. Due to weaker van der Waals forces, 2D materials are more susceptible to pressure than other families of materials. For example, a pressure-induced crossover between indirect and direct bandgaps has been observed in InSe, MoS_2, WS_2, and WSe_2.[5–8] Based on the modulation of the band structure by pressure, an improvement in optoelectronic properties was achieved in many 2D materials. Wang *et al*. have found that pressure may induce a positive to negative photocurrent response switch in $ZrSe_2$ and significantly regulate the optoelectronic properties.[9] Besides, with the help of pressure, many novel properties can be induced which are not available at ambient pressure. By applying pressure on the topological insulator candidate material $Ta_2Pd_3Te_5$, Hui *et al*. observed an emergent superconductivity.[10] The above result shows that pressure has unique advantages in optimizing the properties and discovering novel physical phenomena in 2D materials.

As a typical family of 2D materials, numerous high-pressure studies have been applied to group IVB transition metal dichalcogenides (TMDs). For example, a pressure-induced two-dimensional to three-dimensional (3D) switch was observed in HfS_2, $HfSe_2$, and ZrS_2 following different phase sequences.[11–13] However, whether such a transition belongs to a common feature of group IVB TMDs is still an open question. Besides, although they share the same symmetry at ambient pressure, group IVB TMDs exhibit a rich evolution of the electrical properties during compression which is behind a complex interaction of physical mechanisms.[14–18] In this work, we have performed the structural and electrical transport properties measurements of $ZrSe_2$ under pressure up to 65.5 GPa. Two pressure-induced structural phase transitions were confirmed by high-pressure x-ray diffraction (XRD) and Raman spectroscopic measurement at 8.3 GPa and 31.5 GPa, and phase III belongs to an $I4/mmm$ symmetry relevant to a 3D structure. A pressure-induced metallization was observed in phase II at around 19.4 GPa with a Kondo effect at the low-temperature region. No superconducting transition was observed upon further compression possibly due to the influence of the Kondo effect.

2. Results and discussion

Proportions and element distribution of the single crystal $ZrSe_2$ were analyzed with the scanning electron microscopy (SEM) system equipped with energy dispersive x-ray spectroscopy (EDX). As shown in Fig. S1(a), the SEM spectra reveal a smooth surface of the single crystal $ZrSe_2$. EDX

[†]These authors contributed equally to this work.
[‡]Corresponding author. E-mail: huangxiaoli@jlu.edu.cn

© 2024 Chinese Physical Society and IOP Publishing Ltd

analysis results manifest that the proportions of Zr and Se elements in the single crystal sample are 66.42% and 33.58% [Fig. S1(b)], respectively. Thus, the stoichiometric ratio of the single crystal is $Zr_{1.01}Se_2$, which indicates the high purity of the sample. Figures S1(c)–S1(e) exhibit the elemental distribution map of $ZrSe_2$.

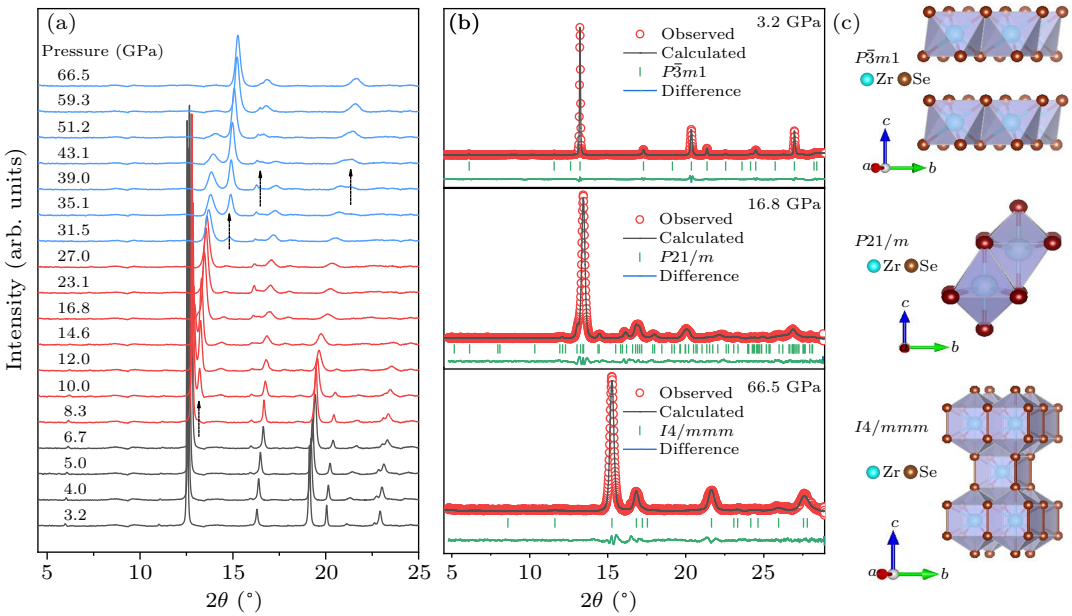


Fig. 1. (a) High-pressure XRD spectra of $ZrSe_2$ ($\lambda = 0.6199$ Å) up to 66.5 GPa. Black arrows indicate the new peaks of phases II and III at 8.3 GPa, 31.5 GPa, and 39.0 GPa. (b) Full-profile Rietveld refinement of phases I, II, and III with *P*-3*m*1, $P2_1/m$, and *I*4/*mmm* symmetries. The red circle points, black solid line, green sticks, and blue solid line represent the experimental data, calculated results, Bragg peaks, and the difference between experimental data and calculated results. (c) Crystal structures of the *P*-3*m*1, $P2_1/m$, and *I*4/*mmm* symmetries of $ZrSe_2$.

$ZrSe_2$ crystallizes in the trigonal *P*-3*m*1 space group at ambient conditions. In this study, high-pressure synchrotron XRD measurements were conducted to explore the structural evolution of $ZrSe_2$ up to 66.5 GPa, as shown in Fig. 1(a). At 3.2 GPa, the XRD measurement result is well fitted using the Rietveld refinement with the *P*-3*m*1 space group, yielding results of $a = b = 3.726$ Å, $c = 5.945$ Å, and $V_0 = 71.477$ Å^3, which are consistent with the previous study.[19] At 8.3 GPa, a new peak appears at $2\theta = 13.17°$, indicating a possible new phase (phase II) at this pressure. As pressure increases from 8.3 GPa to 14.6 GPa, the new peak at $2\theta = 13.17°$ becomes much more intense and gradually replaces the main peak of the initial phase, which indicates a possible mixed state between 8.3 GPa and 14.6 GPa. Above 31.5 GPa, another new phase occurs with three new peaks at $2\theta = 14.9°$, 16.4°, and 21.3°, named phase III. To further confirm the structures of the new phases, we conducted an extensive review of group IVB transition metal dichalcogenides. Previous work has found two possible structures for phase II, which belong to $P2_1/m$ and *Immm* symmetries, respectively. Ghosh *et al*. found that $Zr_{1.03}Se_2$ underwent a gradual structural transition from *P*-3*m*1 to $P2_1/m$ symmetry at 5.9 GPa, while Martino *et al*. suggested that a structural phase transition from *P*-3*m*1 phase to *Immm* phase appeared in $ZrSe_2$ at around 8 GPa.[20,21] As shown in Fig. 1(b), the Rietveld refinement result has shown that the XRD pattern of the sample at 16.8 GPa is in good agreement with the $P2_1/m$ symmetry, thus we believe that a new phase with $P2_1/m$ symmetry at 8.3 GPa is more favorable in our experiment. As for phase III, previous work has predicted a new phase with *I*4/*mmm* symmetry in $ZrSe_2$ after two structural phase transitions during compression,[22] and such an *I*4/*mmm* phase was also predicted in the same family of material ZrS_2.[23]. As shown in Fig. 1(b), the experimental result of *in-situ* XRD measurement at 66.5 GPa is well fitted with *I*4/*mmm* symmetry, thus confirming the third phase of $ZrSe_2$ under pressure. In conclusion, two structural phase transitions from *P*-3*m*1 to $P2_1/m$ (phase II) to *I*4/*mmm* (phase III) symmetry are confirmed in this study from 3.2 GPa to 66.5 GPa. It should be emphasized that for phase III, the *I*4/*mmm* symmetry corresponds to a non-layered structure. Such a 2D to 3D structural phase transition in a layered system is also observed in the same family of materials such as ZrS_2, HfS_2, and $HfSe_2$, which might be regarded as a feature of this family of materials.[11–13]

Lattice parameters as a function of pressure are summarized in Fig. 2(a). To investigate the structural evolution between the three phases, the pressure dependence of volume is fitted based on the third-order Birch–Murnaghan equation of state for the three phases under pressure.[24] As shown in Fig. 2(b), a mixed state of phases I and II is observed between 8.3 GPa and 14.7 GPa, while a mixed state of phases II and III is persistent between 31.5 GPa and 54.9 GPa. The fitted results of V_0, B_0, and B_0' for the three phases are summarized in Fig. 2(b). The volume collapse between phases I and II and between phases II and III is 7% and 12%, respectively.

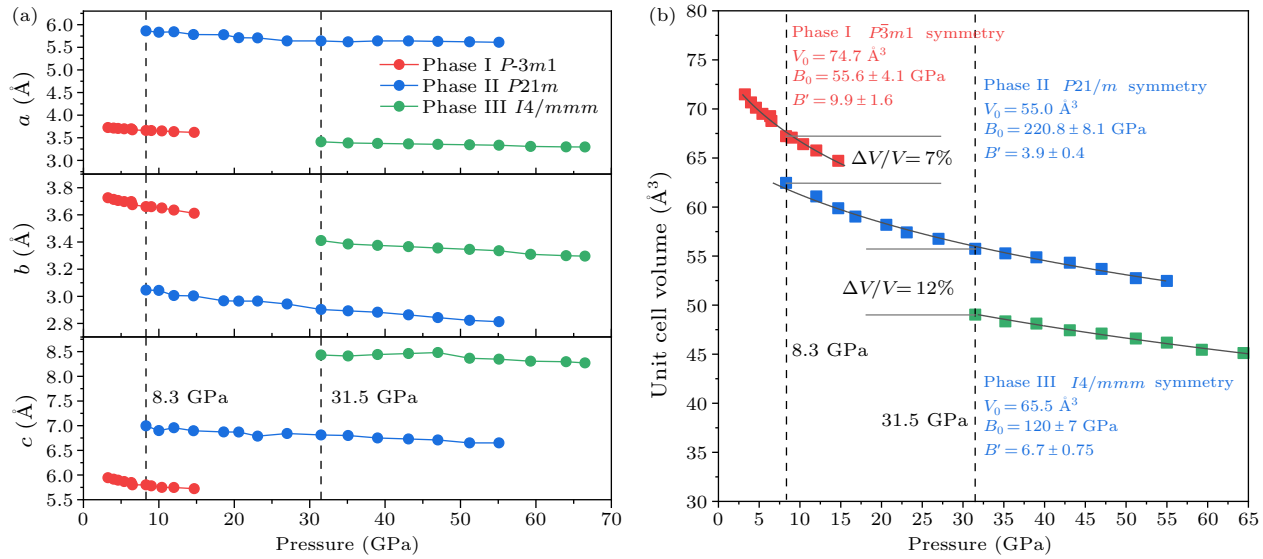


Fig. 2. (a) Lattice parameters of $ZrSe_2$ as a function of pressure. (b) Unit-cell volumes of $ZrSe_2$ as a function of pressure. All three phases are fitted by the third-order Birch–Murnaghan equation of state.

In-situ Raman spectroscopy measurements were conducted at room temperature up to 49 GPa, as shown in Fig. 3(a). At 0.8 GPa, two characteristic peaks are observed in the Raman spectrum of $ZrSe_2$ at 144.5 cm^{-1} and 195.5 cm^{-1}, consistent with previous studies.[25] Peaks at 144.5 cm^{-1} and 195.5 cm^{-1} correspond to the E_g and A_g vibrational modes, representing in-plane and out-of-plane vibrations of Se atoms in $ZrSe_2$, respectively. Figure 3(b) summarizes the pressure-dependent Raman shifts of Raman modes. Both E_g and A_g modes blue-shift in the low-pressure region; the peak shift rate of the A_g mode with pressure (dw/dP) is 12.35 cm^{-1}/GPa, obviously higher than that of the E_g mode 8.95 cm^{-1}/GPa, possibly due to the weak van der Waals forces between layers along the c axis direction. The E_g mode disappears after 7.7 GPa, which may be attributed to the appearance of phase II (for #run 2, at 9.4 GPa), and a change in the peak shift rate of A_g mode is observed at 14.3 GPa, simultaneously with the melting of phase I. The A_g mode retains until 22.3 GPa. As shown in Fig. 3(a), from 11.2 GPa to 14.3 GPa, four new peaks appear at 125.5 cm^{-1}, 166.2 cm^{-1}, 256.9 cm^{-1}, and 274.1 cm^{-1}, as a further evidence of the appearance of phase II, which is consistent with previous results.[26] At 29.8 GPa, a change in the peak shift rate of peak 4 is observed and peak 2 disappears above the pressure, very close to the pressure of the second structural phase transition obtained from the XRD measurement (31.5 GPa). Compared to the result obtained from the XRD measurement (Fig. 2(b)), no clear phase boundary is observed in Fig. 3(b). Considering that Raman shift modes mainly focus on the vibration among different atoms of the sample, we believe that this is a further evidence that the two phase transitions in $ZrSe_2$ belong to a relatively mild phase transition, which means that there are structural similarities between the prior phases and new phases. Therefore, partial inheritance of the original peaks is observed in the Raman spectra measurement.

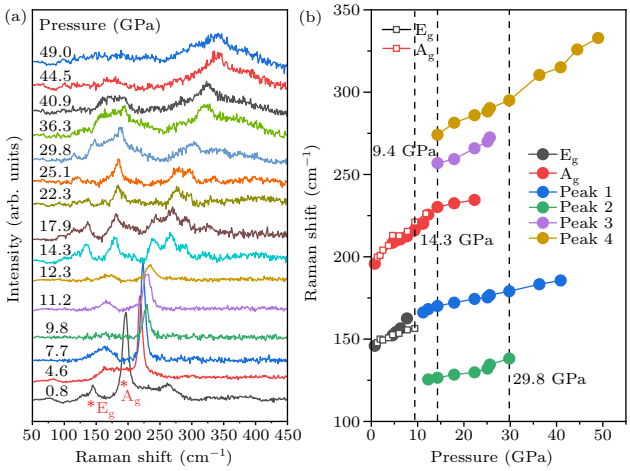


Fig. 3. (a) Raman spectra of $ZrSe_2$ from 0.8 GPa to 49.0 GPa for #run 1. Two characteristic peaks of Raman modes E_g (144.5 cm^{-1}) and A_g (195.5 cm^{-1}) are indicated by red asterisks. (b) Pressure dependence of different Raman modes for both runs, as indicated by solid circles (#run 1) and open squares (#run 2).

Electrical transport measurements were conducted from 2.6 GPa to 64.6 GPa with a standard four-probe method. As shown in Fig. 4, in our experiment, a semiconductor-like behavior is clearly observed from 2.6 GPa to 15.5 GPa. The resistance of the sample decreases by about two orders of magnitude within this pressure range. At 19.4 GPa, a metallic transition is observed in $ZrSe_2$, higher than the pressure range of the mixed state of phases I and II (14.7 GPa). Therefore, the influence of the mixed state on the metallization transition can be excluded. The metallization transition is completed at 30.9 GPa and the resistivity of $ZrSe_2$ is estimated to be 8.0×10^{-7} Ω·m (30.9 GPa, 240 K). Meanwhile, an upturn in resistance is observed in the low-temperature region. In Fig. S2(a), we present the normalized resistance $R/R_{240\ K}$

from 19.4 GPa to 64.6 GPa to get a clearer view of the upturn in the low-temperature region. Such characteristic is also observed in $Zr_{1.03}Se_2$ and the same family of material $ZrTe_2$ and is attributed to the Kondo effect at the low-pressure regions.[20,27] The metallic behavior begins at 19.4 GPa and becomes more and more obvious with increasing pressure up to 64.6 GPa.

To get further insight into the relationship between electrical transport properties and structural phase transitions, pressure-dependent resistances at various temperatures are summarized in Fig. S2(b). All the resistances at different temperatures exhibit a similar trend during compression. One sudden increase in resistance appears between 6.2 GPa and 8.6 GPa, which should originate from the first structural phase transition. Besides, a non-monotonic change in resistance is found at around 9.5 GPa. We believe that such an anomaly is attributed to the mixed state of phases I and II. At the end, a much gentler evolution of resistance is observed above 30.9 GPa, which follows a different slope of phase II, as a further evidence of the appearance of phase III.

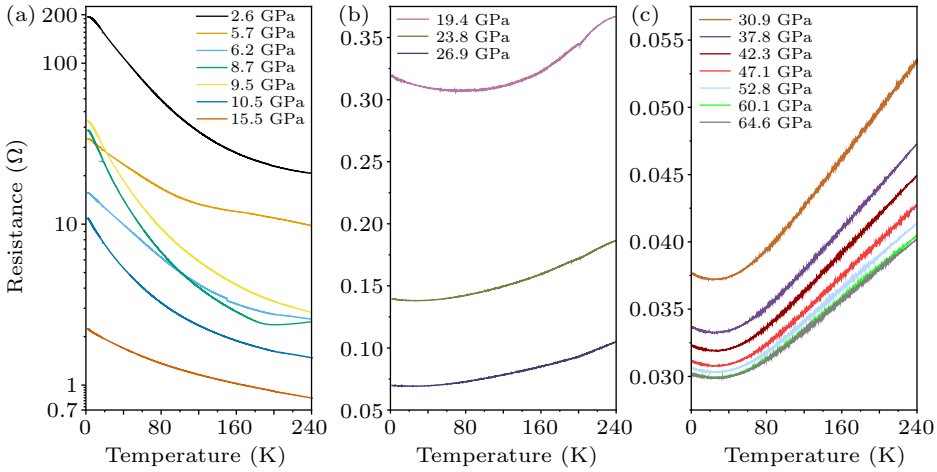


Fig. 4. Electrical transport measurements of $ZrSe_2$ at high pressure. (a) The temperature dependence of resistance for $ZrSe_2$ from 2.6 GPa to 15.5 GPa. (b) The temperature dependence of resistance for $ZrSe_2$ from 19.4 GPa to 26.9 GPa. A metallic behavior is observed above this pressure region. (c) The temperature dependence of resistance for $ZrSe_2$ from 30.9 GPa to 64.6 GPa.

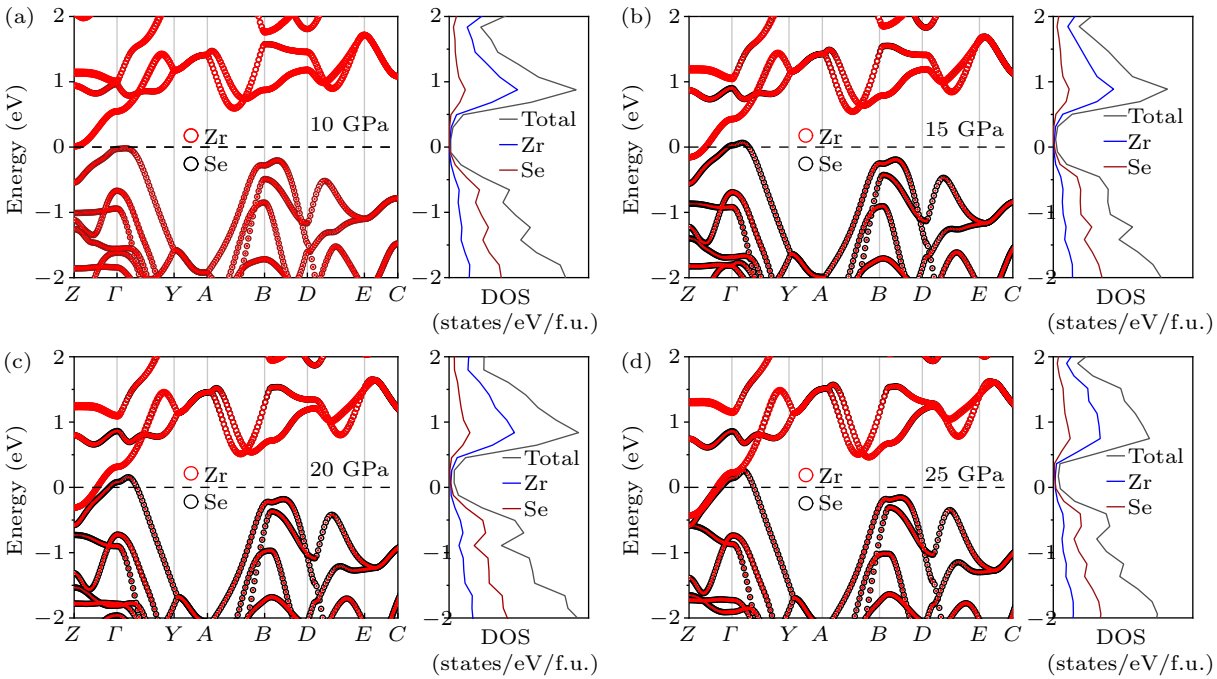


Fig. 5. (a)–(d) Calculated electronic band structure of $P2_1/m$ $ZrSe_2$ from 10 GPa to 25 GPa, together with the high-symmetry points in the corresponding first Brillouin zones. The right panel indicates the total and projected electronic density of states at 10 GPa, 15 GPa, 20 GPa, and 25 GPa, respectively.

To further confirm and explain the metallization transition in phase II, we employed the first-principles calculations on $P2_1/m$ $ZrSe_2$ to determine the band structure and electronic density of states under pressure. As shown in Fig. 5, the results indicate that at 10 GPa, the conduction band and valence band of the $P2_1/m$ phase are located at the Z and Γ points,

respectively, demonstrating a narrow-gap semiconductor with an indirect bandgap of 0.0298 eV, which aligns closely with experimental data. As pressure increases, the conduction band at the Z point shifts downward, while the valence band at the Γ point moves upward. The bandgap closes at 15 GPa, leading to a transition into a metallic state. This trend is consistent with resistance measurements. Further pressure increases result in greater band overlap at the Fermi level.

3. Conclusion

In short, pressure-induced structural phase transitions are observed in $ZrSe_2$ at 8.3 GPa and 31.5 GPa from P-3m1 to $P2_1/m$ and then to $I4/mmm$ symmetry. A mixed state widely exists during compression. The above results, combined with the Raman test results, indicate that two relatively mild phase transitions occur in $ZrSe_2$. The electrical transport study and first-principles calculation results both confirm that phase II appears as a semiconductor phase and is gradually metalized during compression. A pressure-induced 2D to 3D switch occurs during the second structural phase transition. No superconducting state is observed upon further compression possibly due to the influence of the Kondo effect, which appears in the low-temperature region.

Acknowledgments

Project supported by the National Key R&D Program of China (Grant No. 2022YFA1405500) and the National Natural Science Foundation of China (Grant Nos. 52372257 and 52072188). The authors thank the staff of the Beijing Synchrotron Radiation Facility (BSRF) for their help during the synchrotron XRD measurements.

References

[1] Novoselov K S, Geim A K, Morozov S V, Jiang D, Zhang Y, Dubonos S V, Grigorieva I V and Firsov A A 2004 *Science* **306** 666
[2] Wang S, Rehman Z U, Liu Z F, *et al.* 2022 *Chin. Phys. Lett.* **39** 077102
[3] Yan S L, Xie Z J, Chen J H, Taniguchi T and Watanabe K 2017 *Chin. Phys. Lett.* **34** 047304
[4] Wu Y W, Zhang Z Y, Ma L, Liu T, Hao N, Lu W G, Long M S and Shan L 2023 *Chin. Phys. B* **32** 107506
[5] Manjón F J, Errandonea D, Segura A, Muñoz V, Tobías G, Ordejón P and Canadell E 2021 *Phys. Rev. B* **63** 125330
[6] Fu L, Wan Y, Tang N, *et al.* 2017 *Sci. Adv.* **3** e1700162
[7] Luo J H, Li C K, Liu J Y, *et al.* 2024 *Appl. Phys. Lett.* **124** 033104
[8] Gong Y B, Zhou Q, Huang X L, Han B, Fu X P, Gao H X, Li F F and Cui T 2017 *ChemNanoMat* **3** 238
[9] Wang N, Moutaabbid H, Feng Z B, Wang G Y, Zhang H W, Zhang G Z, Cao Z Y, Li Y W and Liu C L 2024 *Appl. Phys. Lett.* **125** 093904
[10] Yu H, Yan D Y, Guo Z P, *et al.* 2024 *J. Am. Chem. Soc.* **146** 3890
[11] Zhong W, Deng W, Hong F and Yue B B 2023 *Phys. Rev. B* **107** 134118
[12] Tian C, Gao Y P, Tian F B, Wang X, Zhang Z H, Duan D F, Huang X L and Cui T 2022 *Phys. Rev. B* **105** L180506
[13] Zhu J, Feng D M, Li L, Zhou Q and Yan Y L 2024 *Phys. Status Solidi B* **261** 2300525
[14] Zhong W, Zhang H, Karaca E, *et al.* 2024 *Phys. Rev. Lett.* **133** 066001
[15] Dutta U, Malavi P S, Sahoo S, Joseph B and Karmakar S 2018 *Phys. Rev. B* **97** 060503
[16] Kusmartseva A F, Sipos B, Berger H, Forró L and Tutiš E 2009 *Phys. Rev. Lett.* **103** 236401
[17] Xia W, Wu J X, Xia C L, *et al.* 2024 *Small* 2402749
[18] Zhu S H, Wu J F, Zhu P, *et al.* 2023 *Adv. Sci.* **10** 2301332
[19] Whitehouse C and Balchin A 1978 *Phys. Status Solidi A* **47** K173
[20] Ghosh B, Sahu M, Samanta D, Saha P, Mondal A and Mukherjee G D 2022 *Phys. Rev. B* **106** 104102
[21] Martino E, Santos-Cottin D, Mardelé F Le, *et al.* 2020 *ACS Mater. Lett.* **2** 1115
[22] Wang S, Du R R, Guo Y L, Sun S T and Ke X Z 2023 *Comp. Mater. Sci.* **226** 112214
[23] Zhai H, Qin Z, Sun D, Wang J Y, Liu C, Min N and Li Q 2018 *Phys. Chem. Chem. Phys.* **20** 23656
[24] Murnaghan F D 1944 *Proc. Natl. Acad. Sci. USA* **30** 244
[25] Mañas-Valero S, García-López V, Cantarero A and Galbiati M 2016 *Appl. Sci.* **6** 264
[26] Ghosh B, Sahu M, Samanta D and Mukherjee G D B 2022 *Mater. Sci.* **45** 221
[27] Wang Y H, Xie C Z, Li J B, *et al.* 2021 *Phys. Rev. B* **103** 174418